

# Mixed-Integer Dynamic Optimization for Oil-Spill Response Planning with Integration of a Dynamic Oil Weathering Model

Fengqi You\* and Sven Leyffer

Argonne National Laboratory, 9700 South Cass Avenue, Argonne, IL 60439

An R&D Note submitted to *AIChE Journal*

**Key words:** MIDO, oil-spill response planning, transport, multi-objective optimization, MINLP

## Introduction

Catastrophic oil spills,<sup>1</sup> such as the recent *Deepwater BP* oil spill in the Gulf of Mexico,<sup>2-3</sup> have demonstrated the importance of developing responsive and effective oil spill response planning strategies for the oil industry and the government. Although a few models have been developed for oil-spill response planning, response operations and the oil weathering process are usually considered separately.<sup>4-6</sup> Yet significant interactions between them exist throughout the response.<sup>6-8</sup> Oil-spill cleanup activities change the volume and area of the oil slick and in turn affect the oil transport and weathering process, which also affects coastal protection activities and cleanup operations (e.g., performance degradation and operational window of cleanup facilities). Therefore, it is critical to integrate the response planning model with the oil transport and weathering model, although this integration has not been addressed in the existing literature to the best of our knowledge.

The objective of this note is to develop an optimization approach for seamlessly integrating the planning of oil-spill response operations with the oil transport and weathering process. A mixed-integer dynamic optimization (MIDO) model is proposed that simultaneously predicts the time trajectories of the oil volume and slick area, the response cleanup schedule and coastal protection plan, by taking into account the time-dependent oil physiochemical properties, spilled amount, hydrodynamics, weather conditions, facility availability, performance degradation, cleanup operational window, and regulatory constraints. To solve the MIDO problem, we reformulated it as a mixed-integer nonlinear programming (MINLP) problem using orthogonal collocation on finite elements. We also developed a mixed-integer linear programming (MILP) model to obtain a good starting point for solving the nonconvex MINLP problem. The application of the proposed integrated optimization approach is illustrated through a case study for an oil spill in Gulf of Mexico. The tradeoff between response cost and the response time span has also been examined and illustrated through the case study.

The rest of this note is organized as follows. The problem statement is presented in the next section. It is then followed by the detailed model formulation and the solution approach. Computational results for a case study and the conclusions are given at the end of this note.

---

\* To whom all correspondence should be addressed. Email: you@northwestern.edu; Tel: 630-252-4669

## Problem Statement

The problem addressed in this work can be formally stated as follows. An oil spill occurs at a specific location. The initial spill volume, constant release rate, and release duration are all known. We are also given the physical and chemical parameters of the oil and seawater, as well as the weather data, such as wind speed and temperature. There is a set of staging areas  $i \in I$  along the shoreline near the spill site. Because of spreading and drift processes, the oil slick may hit the coast around staging area  $i$  at time  $t$  if the slick area is larger than  $\overline{AREA}_{i,t}$ , which is a given parameter in this work and can be derived from the drift process based on weather condition and spill location. A minimum length of boom  $\underline{L}_i$  should be deployed in staging area  $i$  before the oil slick hits the corresponding coast. The maximum boom deployment rates and the unit boom deployment cost are given. Booms deployed around staging area  $i$  will be subject to failure after a lifetime  $\varphi_i$ . The major cleanup methods include mechanical cleanup and recovery (skimming), in-situ burning, and chemical dispersant application; and the corresponding cleanup facilities are indexed by  $m$ ,  $b$ , and  $d$ , respectively. The maximum number of each type of cleanup facility in each staging area and the corresponding total response time are known. The operating capacities of the cleanup facilities and the corresponding operational costs and operating conditions, as well as the time-dependent weather factors, are given. When the response operations finish, the volume of oil remaining on the sea surface should not exceed the cleanup target  $\underline{V}$ . The problem is to simultaneously determine the coastal protection plan and cleanup schedule in order to minimize the total response cost under a specific response time span or to maximize the responsiveness of the operations.

## Mixed-Integer Dynamic Optimization Model

The proposed MIDO model has an objective function to minimize the total response cost, given in (33), and includes a set of ordinary differential equations (ODEs) for the oil transport and weathering process ((1)-(14)) and a set of mixed-integer constraints for response planning ((15)-(32)). The oil weathering model uses a continuous-time representation, while in the planning model we discretize the planning horizon into  $|T|$  time periods with  $H_t$  as the length of time period  $t \in T$ . This is consistent with the real-world practice that most response decisions are made on an hourly or daily basis. The integration of these two time representations will be discussed in Section 4. A list of indices, parameters, and variables is given in the nomenclature section.

### Oil transport and weathering model

Prediction of the oil transport and weathering process needs to account for many factors, such as oil properties, spilled amount, hydrodynamics, and weather conditions, and to consider a variety of complex

physicochemical processes taking place simultaneously (see Figure 1). Over 50 oil weathering models, based on empirical and semi-empirical approaches, have been developed. Although any oil weathering model can, in principle, be used in the approach proposed in this paper, we employ a dynamic mathematical model taking into account the dominant processes (spreading, evaporation, emulsification, and dispersion) that cause significant short-term changes in oil characteristics, as the focus of this work is to integrate response planning model and dynamic oil weathering model. We note that a PDE model might better capture the physiochemical evolution of oil slick in the three dimension space, it might be challenging to be integrated with the response planning model. Thus, we consider only the time variation in area, volume and other important physiochemical parameters, and model the effects of wind and current through parameters with constant values.

Spreading, which strongly influences coastal protection operations and other weathering processes, is probably the most dominant process of a spill. The rate of change of slick area is given by<sup>9-11</sup>

$$\frac{dA_{(t)}}{dt} = K_1 A_{(t)}^{-1} V_{(t)}^{4/3} - W_{(t)} \cdot \frac{A_{(t)}}{V_{(t)}} , \quad (1)$$

where  $A$  is the surface area of oil slick,  $V$  is the volume of oil,  $K_1$  is the empirical physicochemical parameters of the crude oil, and  $W$  is the cleanup rate given in Equation (32). The first term on the right-hand side of Equation (1) is for the natural spreading process. The second term refers to the reduction of slick area as a result of cleanup operations. Symbols with subscript  $(t)$  are time-dependent variables.

The initial area of oil slick can be determined by the well-known gravity-viscous formulation:<sup>12</sup>

$$A_0 = \pi \frac{k_2^4}{k_3^2} \left[ \frac{(\rho_w - \rho_o) g V_0^5}{\rho_w \nu_w} \right]^{1/6} , \quad (2)$$

where  $g$  is the acceleration of gravity ( $\text{m} \cdot \text{s}^{-2}$ ),  $\rho_w$  is seawater density,  $\rho_o$  is the density of fresh oil,  $\nu_w$  is the kinematic viscosity of seawater,  $V_0$  is the initial volume, and  $k_2$  and  $k_3$  are empirical constants.

The volume balance of the oil slick is based on the volume variation rate given as follows:<sup>11, 13</sup>

$$\frac{dV_{(t)}}{dt} = -V_{(t)} \frac{dF_{E(t)}}{dt} - \frac{dV_{D(t)}}{dt} - W_{(t)} + VI_{(t)} , \quad (3)$$

where the first term on the right-hand side is for the evaporation loss, the second term is for natural dispersion, the third term is the cleanup rate, and the last term is the oil release rate given as follows:<sup>11</sup>

$$VI_{(t)} = \begin{cases} \text{constant release rate,} & 0 \leq t \leq tf_1 \\ 0, & tf_1 \leq t \leq tf_2 \end{cases} , \quad (4)$$

where  $tf_1$  is the time when the oil spillage stops and  $tf_2$  is the final time of the planning horizon (response time span). The initial volume of the oil slick is given as  $V_0$ , and the remaining volume of oil at the end of the response time span should not exceed the cleanup target.

$$V_{(t=0)} = V_0 \text{ and } V(t = tf2) \leq \underline{V} \quad (5)$$

Evaporation is the primary initial process involved in the removal of oil from sea. The rate that oil evaporates from the sea surface is modeled by the following equation:<sup>14</sup>

$$\frac{dF_{E(t)}}{dt} = \frac{K_{ev} A_{(t)}}{V_{(t)}} \exp\left(A_{ev} - \frac{B_{ev}}{T_K} (T_o + T_G F_{E(t)})\right), \quad (6)$$

where  $F_E$  is the volume fraction of oil that has been evaporated,  $T_K$  is the oil temperature, which is assumed to be a constant,  $K_{ev}$  is the mass transfer coefficient for evaporation with an empirical value equals to  $2.5 \times 10^{-3} \cdot WIND^{0.78}$  ( $WIND$  is the wind speed),<sup>15</sup>  $T_o$  is the initial boiling point,  $T_G$  is the gradient of the oil distillation curve, and  $A_{ev}$  and  $B_{ev}$  are empirical constants. As no oil was evaporated at time 0, the initial value of evaporative fraction is given by

$$F_{E(t=0)} = 0. \quad (7)$$

The rate of dispersion into the water column of the floating oil slick is given by the following:<sup>9-10, 13</sup>

$$\frac{dV_{D(t)}}{dt} = \frac{0.11 \cdot (WIND + 1)^2 \cdot A_{(t)} \cdot V_{(t)}}{A_{(t)} + 50 \zeta_t \cdot V_{(t)} \cdot \mu_{(t)}^{1/2}}, \quad (8)$$

where  $V_D$  is volume of oil naturally dispersed, and  $\zeta_t$  is the oil-water interfacial tension. The initial value of the volume of oil that is naturally dispersed is zero.

$$V_{D(t=0)} = 0 \quad (9)$$

In emulsification, water droplets are entrained in the oil. The dynamic emulsification process that incorporates water into oil can be computed with the following equation:<sup>9</sup>

$$\frac{dY_{W(t)}}{dt} = K_{em} \cdot (WIND + 1)^2 \cdot \left(1 - \frac{Y_{W(t)}}{C_3}\right), \quad (10)$$

where  $Y_W$  is the fractional water content in the emulsion,  $C_3$  is a viscosity constant for the final fractional water content, and  $K_{em}$  is an empirical constant. The initial value of  $Y_W$  can be approximated to zero:

$$Y_{W(t=0)} = 0. \quad (11)$$

Equations (10) and (11) yield the dynamic fractional water content of the oil slick as follows:

$$Y_{W(t)} = C_3 \cdot \left[1 - \exp\left(-\frac{K_{em}}{C_3} \cdot (WIND + 1)^2 \cdot t\right)\right]. \quad (12)$$

As a result of both Mousse formation (emulsification with seawater) and evaporation, the viscosity of oil slick may significantly increase during the weathering process. The rate of changes in viscosity is given by<sup>13, 15</sup>

$$\frac{d\mu_{(t)}}{dt} = \frac{2.5\mu_{(t)}}{(1 - C_3 Y_{W(t)})^2} \frac{dY_{W(t)}}{dt} + C_4 \mu \frac{dF_{E(t)}}{dt}, \quad (13)$$

where  $\mu$  is the viscosity of the oil slick and  $C_4$  is an oil-dependent empirical constant.

The initial value of the viscosity is the same as that of the parent oil viscosity, which can be calculated by the following equation:<sup>15</sup>

$$\mu_0 = 224 \times \sqrt{AC}, \quad (14)$$

where  $AC$  is the asphaltene content (%) of the parent oil.

As this dynamic model is based on semi-empirical approach, the accuracy of its prediction largely depends on the empirical parameters. We note that cleanup rate  $W_{(t)}$  is the only major control variable of this problem. The reader can refer to the work by Zhong and You<sup>11</sup> for the dynamic response the oil weathering model to changes of cleanup rate.

### Oil spill response planning constraints

We consider both coastal protection and oil-spill cleanup operations in the response. The major coastal protection method is to deploy booms to prevent the oil from spreading to the shore. Three major oil spill cleanup methods are mechanical cleanup and recovery, in-situ burning, and chemical dispersants. Mechanical systems can skim the oil slick and recover oil from the emulsion; in-situ burning and chemical dispersants only remove oil from the surface of the sea. Reviews of oil spill response methods and equipment are given by Ventikos et al.<sup>16</sup> and Zhong.<sup>11</sup>

In order to protect sensitive shorelines, either the slick area must be controlled through effective cleanup operations, or coastal protection booms must be deployed with sufficient lengths around those staging areas before the oil slick reaches them. The following constraint models this relationship:

$$A_{(t)} \leq \overline{AREA}_{i,t} + A^U \cdot z_{i,t} \quad \forall i \in I, t \in T, \quad (15)$$

where  $z_{i,t}$  is a binary variable that equals to 1 if sufficient booms have been deployed to protect the shoreline around staging area  $i$  at time  $t$ ,  $A^U$  is the upper bound of oil slick area, and  $\overline{AREA}_{i,t}$  is a given parameter for the area of the oil slick that will hit the shore around staging area  $i$  at time period  $t$ .  $\overline{AREA}_{i,t}$  depends primarily on the drift process, which relates to the wind speed and direction.<sup>11</sup>

The shoreline around staging area  $i$  is fully protected by the booms at time period  $t$  if and only if the length of boom is no less than the required length. So we have

$$\underline{L}_i \cdot z_{i,t} \leq bl_{i,t} \leq \underline{L}_i + bl^U \cdot z_{i,t} \quad \forall i \in I, t \in T, \quad (16)$$

where  $\underline{L}_i$  is the length of boom required to protect the coast around staging area  $i$  and  $bl_{i,t}$  is the length of boom deployed along the shore of staging area  $i$  at the end of time period  $t$ , and  $bl^U$  is its upper bound.

Because of currents and winds, conventional booms are subject to damages over time. Coastal protection booms deployed at staging area  $i$  can be effective for only a certain lifetime  $\varphi_i$  after deployment. Booms deployed at time  $t - \varphi_i$  will fail at time  $t$ .<sup>8</sup>

$$bfail_{i,t} = bdep_{i,t-\varphi_i} \quad \forall i \in I, t \geq \varphi_i + 1 \quad (17)$$

The length of the boom around the shore of staging area  $i$  at the end of time period  $t$  ( $bl_{i,t}$ ) is equal to the boom length at the end of the previous time period ( $bl_{i,t-1}$ ) plus the length of the boom deployed at the current time period ( $bdep_{i,t}$ ) minus those that fail at this time period ( $bfail_{i,t}$ ). Thus, the balance of boom length is given by the following equation.

$$bl_{i,t} = bl_{i,t-1} + bdep_{i,t} - bfail_{i,t} \quad \forall i \in I, t \in T \quad (18)$$

The length of boom deployed along the shoreline near staging area  $i$  at time  $t$  should not exceed the maximum deployment rates ( $BDU_{i,t}$ ) times the length of time period  $t$  ( $H_t$ ). Thus, we have

$$bdep_{i,t} \leq BDU_{i,t} \cdot H_t \quad \forall i \in I, t \in T, \quad (19)$$

We define  $x_{i,m,t}^M$  as the number of mechanical systems  $m$  from staging area  $i$  operating at the scene at time period  $t$ . It should not exceed the corresponding available number ( $N_{i,m}^M$ ). None of the mechanic systems can operate before the response time ( $\lambda_{i,m}^M$ ) to notify, mobilize, dispatch, and deploy them.

$$x_{i,m,t}^M \leq N_{i,m}^M \quad \forall i \in I, m \in M, t \in T \quad (20)$$

$$x_{i,m,t}^M = 0 \quad t \leq \lambda_{i,m}^M \quad (21)$$

The volume of oil cleaned and recovered from the sea surface with mechanical systems at time period  $t$  ( $WM_t$ ) is given by the following equation.<sup>6</sup>

$$WM_t = \sum_i \sum_m \left(1 - Y_{W(t)}\right) \cdot H_t \cdot \omega_t^M \cdot Q_{i,m}^M \cdot x_{i,m,t}^M \quad \forall t \in T, \quad (22)$$

where  $Q_{i,m}^M$  is the operating capability of mechanical system  $m$  from staging area  $i$ ;  $\omega_t^M$  is the weather factor (between 0 and 1), which can be determined from weather forecasting; and  $Y_{W(t)}$  is the fractional water content defined in (12).

In-situ burning response system  $b$  can operate only when the oil slick ( $\delta_t$ ) is thicker than  $THICK_b$ .<sup>7</sup>

We introduce a binary variable ( $xx_{b,t}^B$ ) to model this restriction through the following constraint:

$$THICK_b \cdot xx_{b,t}^B \leq \delta_{(t)} \leq THICK_b + THICK^U \cdot xx_{b,t}^B \quad \forall i \in I, b \in B, t \in T \quad (23)$$

where  $THICK^U$  is the upper bound of the slick thickness and  $\delta_{(t)}$  is the thickness of the oil slick given by

$$\delta_{(t)} \cdot A_{(t)} = V_{(t)} \quad (24)$$

For in-situ burning response systems, the availability constraints are given as follows:

$$x_{i,b,t}^B \leq N_{i,b}^B \cdot xx_{b,t}^B \quad \forall i \in I, b \in B, t \in T \quad (25)$$

$$x_{i,b,t}^B = 0 \quad t \leq \lambda_{i,b}^B, \quad (26)$$

where  $x_{i,b,t}^B$  is the number of in-situ burning systems  $b$  from staging area  $i$  operating at the scene at time period  $t$ ,  $N_{i,b}^B$  is the available number in staging area  $i$ , and  $\lambda_{i,b}^B$  is the corresponding response time.

The volume of oil burned at time period  $t$  ( $WB_t$ ) is given by the following equation:

$$WB_t = \sum_i \sum_m H_t \cdot \omega_t^B \cdot Q_{i,b}^B \cdot x_{i,b,t}^B \quad \forall t \in T, \quad (27)$$

where  $Q_{i,b}^B$  is the operating capability of in-situ burning system  $b$  from staging area  $i$  and  $\omega_t^B$  is the weather factor for in-situ burning operations at time  $t$ .

The availability constraint of chemical dispersant application systems is given by

$$x_{i,d,t}^D \leq H_t \cdot \gamma_{i,d,t} \cdot N_{i,d}^D \quad \forall i \in I, d \in D, t \in T, \quad (28)$$

$$x_{i,d,t}^D = 0 \quad t \leq \lambda_{i,d}^D \quad (29)$$

where  $x_{i,d,t}^D$  is the number of sorties of chemical dispersant application systems  $d$  dispatched from staging area  $i$  at time period  $t$ ,  $N_{i,d}^D$  is the corresponding availability, and  $\gamma_{i,d,t}$  is the maximum number of sorties of dispersant application systems  $d$  from staging area  $i$  to spray dispersant on the oil slick at time period  $t$ . Note that the maximum number of sorties depends on the type of dispersant application system (e.g., a helicopter may operate 10 sorties per day for an offshore oil spill 100 miles away).<sup>17</sup>

The volume of oil removed from the sea surface by using chemical dispersants at time period  $t$  ( $WD_t$ ) is given by the following equation:

$$WD_t = \sum_i \sum_d \omega_t^D \cdot \rho_t^{effect} \cdot \rho_d^{accuracy} \cdot Q_{i,d}^D \cdot x_{i,d,t}^D \quad \forall t \in T, \quad (30)$$

where  $Q_{i,d}^D$  is the operating capacity of dispersant application systems  $d$  from staging area  $i$ ,  $\omega_t^D$  is the corresponding weather factor,  $\rho_t^{effect}$  is the effectiveness factor (ratio between oil dispersed and dispersant sprayed) for chemical dispersant application at time  $t$ , and  $\rho_d^{accuracy}$  is the accuracy factor (percentage of sprayed dispersant that can reach the oil slick) of dispersant application systems  $d$ .

The total amount of chemical dispersant used throughout the entire response operation should be constrained by the government regulation ( $DLIMIT$ ).<sup>17</sup>

$$\sum_i \sum_d \sum_t Q_{i,d}^D \cdot x_{i,d,t}^D \leq DLIMIT \quad (31)$$

We model the real-time cleanup rate ( $W_{(t)}$ ) as a piece-wise step function as follows:

$$W_{(t)} \cdot H_t = WM_t + WB_t + WD_t. \quad (32)$$

Note that different cleaning operations can be performed simultaneously, as there is no sequencing issues related to the three cleanup types of cleanup methods.

## Objective functions

The objective function is to minimize the total response cost, given as follows.

$$\begin{aligned} \min : TotalCost = & \sum_i \sum_m \sum_t C_{i,m,t}^M \cdot x_{i,m,t}^M + \sum_i \sum_b \sum_t C_{i,b,t}^B \cdot x_{i,b,t}^B + \sum_i \sum_b \sum_t C_{i,d,t}^D \cdot x_{i,d,t}^D \\ & + \sum_i \sum_t CDEP_{i,t}^{boom} \cdot bdep_{i,t} - \sum_t WM_t \cdot OC \end{aligned} \quad (33)$$

Here the first three terms are the cost of the cleanup operations, the fourth terms is the cost of coastal protection operations, and the last term is the credit resulting from the recovery of the emulsified oil. We note that another possible objective of this problem is to minimize the time span of the entire response

operations,<sup>11</sup> which is a measure of responsiveness.<sup>18-20</sup>

## Solution Approach

A number of approaches exist for solving MIDO problems.<sup>21-24</sup> Because of the problem size and structure, in this work we use a simultaneous approach, the robustness and efficiency of which have been demonstrated by a number of large-scale applications in process control and operations.<sup>25-30</sup>

### Simultaneous approach for solving the MIDO problem

In the simultaneous approach,<sup>21</sup> the MIDO model is fully discretized based on orthogonal collocation on finite elements and then is reformulated into an equivalent MINLP problem. First, the entire planning horizon is divided into a number of finite elements. Within each finite element an adequate number of internal collocation points is selected. Using several finite elements is useful to represent dynamic profiles with nonsmooth variations. Thus, the differential and algebraic variable profiles are approximated at each collocation point by using a family of interpolation polynomials.

To integrate the continuous- and discrete-time representations in the model, we consider one time period as a finite element in the discretization process. In this way, the index  $t$  represents not only the discrete time periods but also the finite elements, and the length of finite element  $t$  is the same as the length of the corresponding time period ( $H_t$ ). In this section we use the symbol  $S$  to generically represent the differential variables  $A_{(t)}$ ,  $F_{E(t)}$ ,  $\mu_{(t)}$ ,  $V_{D(t)}$ , and  $V_{(t)}$ . Then, in the discretization process, differential equations (1), (6), (13), (8), and (3) are replaced with the following generic equations:

$$S_{t,p} = S0_t + H_t \sum_{p'=1}^{|P|} \Omega_{p',p} \cdot \dot{S}_{t,p}, \quad \forall t \in T, p \in P, \quad (34)$$

$$S0_t = S0_{t-1} + H_{t-1} \sum_{p=1}^{|P|} \Omega_{p,p'=|P|} \cdot \dot{S}_{t-1,p}, \quad \forall t \in T, \quad (35)$$

$$\dot{S}_{t,p} = f\left(A_{(t)}, F_{E(t)}, \mu_{(t)}, V_{D(t)}, V_{(t)}, W_{(t)}\right) \quad \forall t \in T, p \in P, \quad (36)$$

where  $S_{t,p}$  is the value of the state in finite element  $t$  and collocation point  $p$ ,  $S0_t$  is the state value at the beginning of finite element  $t$ ,  $\dot{S}_{t,c}$  is the first-order derivative of the state, and  $\Omega_{p',p}$  is the collocation matrix. Radau collocation points are used in this work because they stabilize the system more efficiently in the presence of high-index differential algebraic equations. Equation (34) is used to compute the value of the system states at each discretized point  $S_{t,p}$  by using the monomial basis representation. Equation (35) is to enforce the continuity of the differential profiles across finite elements. Equation (36) simply represents the right-hand side of the dynamic model for computing the value of the first-order derivatives of the systems.

The initial and final conditions in (2), (7), (14), (9), and (5) are replaced by the following equations:

$$S0_{t=1} = S_0. \quad (37)$$



$$S_{t=tf_2, p=|P|} = S_{tf_2} . \quad (38)$$

The time value of each collocation point in each finite element is given by

$$TIME_{t,p} = \sum_{t'=1}^{t'-t-1} H_{t'} + H_t \cdot \Psi_p \quad \forall t \in T, p \in P, \quad (39)$$

where  $\Psi_p$  is the roots of the Lagrange orthogonal polynomial. This equation can be used to calculate the fractional water content in Equation (12).

After the reformulation the differential equations are discretized as in Equations (34)–(39), and the resulting problem is a nonconvex MINLP with nonlinear terms in (22), (24), and (36).

### Approximate MILP model for initialization

The simultaneous approach requires careful initializations and might suffer from numerical difficulties associated with the nonlinear nonconvex terms in the reformulated MINLP. To obtain a “good” starting point, we developed an MILP model for initialization. The approximate MILP model, which is obtained by decoupling the ODE from the discrete-time response planning model, implicitly considers the oil weathering process in the response planning by assuming the time trajectory of the slick thickness is not affected by response operations.<sup>11</sup> First, we use the Runge–Kutta method to solve the ODE-based oil weathering model without considering response operations, that is, natural weathering with zero cleanup rate ( $W_{(t)} = 0$ ). The oil volume, slick area, and water content predicted by the ODE model are denoted as  $V^*(t)$ ,  $A^*(t)$ , and  $Y_W^*(t)$ , respectively. Then, at each discrete time period the slick thickness can be calculated by  $\delta_t^* = V^*(t)/A^*(t)$ . We further define  $\theta_t$  as the percentage of oil removed from the slick at time period  $t$  by natural weathering. Its value can be calculated by  $\theta_t = [V^*(t-1) - V^*(t) + VI_t \cdot H_t]/V^*(t-1)$ , where the term  $(VI_t \cdot H_t)$  accounts for the volume of oil newly released to the sea surface in time period  $t$ .

The MILP model has the same objective function given in Equation (33). The model also includes the following constraints for slick area, volume balance, and cleanup target, respectively:<sup>11</sup>

$$v_t = area_t \cdot \delta_t^*, \quad \forall t \in T, \quad (40)$$

$$V_0 + VI_{t=1} \cdot H_{t=1} = v_{t=1} + \theta_{t=1} \cdot V_0 + W_{t=1}^M + W_{t=1}^B + W_{t=1}^D, \quad (41)$$

$$v_{t-1} + VI_t \cdot H_t = v_t + \theta_t \cdot v_{t-1} + W_t^M + W_t^B + W_t^D, \quad \forall t \geq 2, \quad (42)$$

$$v_{t=tf_2} \leq \underline{V}, \quad (43)$$

where  $v_t$  and  $area_t$  are the volume and area of the oil slick at the end of the discrete time period  $t$ , respectively.

The rest of constraints in the MILP model include (15) - (23) and (25) - (32). Note that the fractional water content  $Y_{W(t)}$  in Equation (22) and the slick thickness  $\delta_{(t)}$  in Equation (23) are fixed to  $Y_W^*(t)$  and  $\delta_t^*$ , respectively.

## Case Study: Oil Spill in the Gulf of Mexico

Our case study is based on an oil spill in the Gulf of Mexico. There are three major staging areas for the response operations: S1, S2, and S3. Their locations, along with the spill site, are given in the map in Figure 3. The minimum distances between the three staging areas and the oil spill site are 60 kilometers, 120 kilometers, and 180 kilometers, respectively. The maximum boom deployment rates at the three staging areas are 25km/day, 21km/day and 22km/day, respectively. The life times of coastal protection booms at the three staging areas are 100 days, 130days and 120 days, respectively. In this case, we assume the oil slick drifts toward the shore as a result of wind and current directions. The lengths of the booms required to protect the sensitive coastline near the three staging areas are 200 kilometers, 180 kilometers, and 300 kilometers, respectively. The spilled oil is considered as crude oil with an API degree of 25, an initial boiling point of 439K and the gradient of the oil distillation curve of 970K. The Oil-water interfacial tension is  $0.02 \text{ N}\cdot\text{m}^{-1}$ . The initial spill amount is  $10,000 \text{ m}^3$ , and the oil releases continue for 42 days with a constant rate of  $10,000 \text{ m}^3/\text{day}$ . The cleanup target is that no more than  $1,500 \text{ m}^3$  of oil remain on the sea surface after the response. The cleanup facilities include three types of mechanical systems, two types of in-situ burning systems, and three types of dispersant application systems. The operating capacity, availability, and response time of each type of cleanup faculties are listed in Table 1.

All the computational studies were performed on an IBM T400 laptop with an Intel 2.53 GHz CPU and 2 GB RAM. DICOPT was used as the MINLP solver. The MILP problems were solved by using CPLEX 12.2 with an optimality tolerance of  $10^{-9}$ . The nonlinear programming subproblems were solved with the KNITRO solver with an optimality tolerance of  $10^{-6}$ . In order to examine the trade-off between the total cost and the responsiveness, which is measured by the response time span,<sup>11</sup> we need to solve a large-scale non-convex multi-objective MINLP. Although a global optimal solution of this problem might be intractable, we use  $\varepsilon$ -constraint method to obtain an approximation of the Pareto curve. We consider one day as a time period or a finite element. Because the oil volume will reduce to the cleanup target ( $1,500 \text{ m}^3$ ) in 180 days without cleanup actions (i.e., natural weathering) and setting the response time span less than 76 days usually leads to an infeasible solution, we solve 105 instances with a response time span ranging from 76 days to 180 days, with increments of one day. The maximum MINLP problem with a response time span of 180 days includes 2,052 discrete variables, 11,482 continuous variables, and 14,006 constraints. For each instance, we first solve the approximate MILP problem and use its solution as the starting point of solving the MINLP problem. The solution process takes a total of 15,059 CPU-seconds for all 105 instances. We note that the problem becomes “infeasible”, when we solved the MINLP directly or using multiple starting point strategy without the initialization step.

The results are given in Figures 4–11. The line in Figure 4 is the “local-optimal” Pareto curve of this problem. We can see that as the response time span increases from 76 days to 180 days, the total cost decreases from \$998 million to \$54 million. Thus, the more responsive the response operation is, the more it costs. In particular, when the response time span increases from 76 days (Point A) to 78 days (Point B), the total cost reduces almost by half. This suggests that 78 days might be a better choice for the oil spill response based on the trade-off between economics and responsiveness. The pie charts in Figure 4 are for the breakdown of the total costs for Points A–F. We can see that as the time span increases and the total cost decreases, more and more is spent on coastal protection. The reason is that the least-cost option for this case study is to deploy booms to protect the sensitive shorelines while leaving the oil slick on the sea surface until natural weathering reduces the oil volume to the cleanup target; that is, no cleanup efforts are taken in the least-cost instance.

Figures 5–7 show the time trajectories of the oil volume throughout the response operations for the Points A–C in Figure 4, where time spans are 76 days, 78 days, and 95 days. The drop lines are for the collocation points in the finite elements. We can see a similar trend from these figures that the volume of remaining oil first increases from Day 0 to Day 42 and then decreases, because the oil was being released at a constant rate to the sea surface before Day 42. These figures reveal that the more cleanup operations are taken, the earlier the cleanup target can be achieved. They also show that dispersant application is usually the most favorable cleanup method because of its flexibility in various weather conditions, although it needs longer response time than other methods. In the shortest time span instance, however, skimming becomes as important as dispersant application, because the total amount of chemical dispersant used is constrained by regulation and mechanical cleanup can gain credit from oil recovery. The time trajectories of the oil volume and area when response time span is 180 days (Point F in Figure 4) are given in Figure 8. As no cleanup effort was taken in this instance, the time trajectories are the same as those for natural weathering process.

Figure 9 shows the length of coastal protection booms deployed in the three staging areas when the response time span is 76 days. We can see that the three staging areas start to deploy booms from Day 8, Day 21, and Day 19, respectively. The different starting days are due to the different boom deployment rates and different locations of the staging areas. S1 deploys the booms first, because it has the shortest distance to the oil spill site; Although S2 is closer to the spill site than S3, S3 starts to deploy the booms earlier than S2, because S3 requires much longer booms to protect the coast and longer deployment time.

## Conclusion

In this paper, we have developed an MIDO approach for oil spill response planning with integration of the physiochemical evolution of oil slicks. The MIDO model includes a dynamic oil weathering

model, which takes into account time-dependent oil properties, spilled amount, hydrodynamics, and weather conditions, and models the complex interactions between the spreading, evaporation, dispersion, and emulsification processes. In addition to the time trajectories of oil volume and slick area, the MIDO model simultaneously predicts the optimal coastal protection plans and oil spill cleanup schedule with different types of mechanic, burning, and dispersant application equipments. The MIDO model was reformulated to a MINLP problem after full discretization, and an approximate MILP model was developed for the initialization of solving the large-scale, nonconvex MINLP. An example was presented to illustrate the application of the proposed integrated optimization approach. The results demonstrate the importance of integrating an oil transport and weathering model in response planning.

This work can be extended to deal with the uncertainty involved in the model. There are two potential approaches that can effectively tackle this issue. One is to extend the MIDO model to its stochastic version and to explicitly consider these uncertain parameters; the other is to apply a real time MIDO formulation. Another possible future work is to develop an efficient method to quantify the cost due to the damages caused by an oil spill to the marine ecosystem and to the local economy, and include it in the model for a better tradeoff between the economics and responsiveness.

## Acknowledgment

This research is supported by the U.S. Department of Energy under contract DE-AC02-06CH11357.

## Nomenclature

### Nomenclature for the planning model

#### Sets/Indices

$B$	Set of in-situ burning response system types indexed by $b$
$D$	Set of chemical dispersant application system types indexed by $d$
$I$	Set of staging areas (including airlift wing stations) indexed by $i$
$M$	Set of skimming (mechanical cleanup & recovery) system types indexed by $m$
$P$	Set of collocation points indexed by $p, p'$
$T$	Set of time periods/finite elements indexed by $t, t'$

#### Parameters

$\overline{AREA}_{i,t}$	Expected slick area that the oil slick would hit the shore around staging area $i$ at time period $t$ if no boom in this area was deployed for protection ( $m^2$ )
$BDU_{i,t}$	Maximum deployment rate of boom in staging area $i$ at time period $t$ (m/day)
$C_{i,m,t}^M$	Operating cost of mechanical cleanup and recovery system $m$ from staging area $i$ at time $t$ (\$/time period)
$C_{i,b,t}^B$	Operating cost of in-situ burning system type $b$ from staging area $i$ at time $t$ (\$/time period)
$C_{i,d,t}^D$	Cost of dispatching a chemical dispersant application system $d$ from staging area $i$ at time $t$ to spray a full-load dispersant (\$/sortie)
$CDEP_{i,t}^{boom}$	Cost of deploying unit length of coastal protection boom in staging area $i$ (\$/m)
$DLIMIT$	Maximum amount of dispersant that can be applied in the cleanup ( $m^3$ )

$H_t$	Length of time period $t$ (day/time period)
$\underline{L}_i$	Length of boom required to protect the shore around staging area $i$ (m)
$N_{i,b}^B$	Available number of in-situ burning response systems of type $b$ in staging area $i$
$N_{i,d}^D$	Available number of chemical dispersant application systems of type $d$ in staging area $i$
$N_{i,m}^M$	Available number of mechanic systems of type $m$ that can be dispatched from staging area $i$
$OC$	Unit price of recovered oil (\$/m <sup>3</sup> )
$THICK_b$	Minimum slick thickness that in-situ burning response system $b$ can operate (m)
$Q_{i,b}^B$	Operating capability of in-situ burning system $b$ from staging area $i$ (m <sup>3</sup> /day)
$Q_{i,d}^D$	Full load capacity of dispersant application system $d$ from staging area $i$ (m <sup>3</sup> /sortie)
$Q_{i,m}^M$	Operating capability of mechanical cleanup system $m$ from staging area $i$ (m <sup>3</sup> /day)
$TIME_{t,p}$	Value of time at collocation point $p$ in finite element $t$
$V_0$	Initial volume of oil spilled at time 0 (m <sup>3</sup> )
$VI_t$	Volume of oil that was newly released to the sea surface at time $t$ (m <sup>3</sup> )
$\underline{V}$	Cleanup target, maximum volume of oil left on the sea surface after cleanup (m <sup>3</sup> )
$\rho_t^{effect}$	Effectiveness factor (ratio between oil dispersed and dispersant sprayed) for chemical dispersant application operation at time $t$
$\rho_d^{accuracy}$	Accuracy factor (percentage of sprayed dispersant that can reach oil slick) of chemical dispersant application system $d$
$\lambda_{i,b}^B$	Total response time of in-situ burning response system type $b$ dispatched from staging area $i$ (including times to notify, mobilize, dispatch, and deploy the system) (m <sup>3</sup> )
$\lambda_{i,d}^D$	Total response time of chemical dispersant system types $d$ dispatched from staging area $i$
$\lambda_{i,m}^M$	Total response time of mechanic cleanup and recovery system type $m$ from staging area $i$
$\omega_t^M$	Weather factor for mechanic cleanup and recovery operation at time $t$
$\omega_t^B$	Weather factor for controlled burning operation at time $t$
$\omega_t^D$	Weather factor for chemical dispersant application operation at time $t$
$\gamma_{i,d,t}$	Maximum number of sorties of dispersant application system types $d$ from staging area $i$ to oil spill site in time period $t$
$\phi_i$	Lifetime before failure for containment booms deployed at staging area $i$
$\eta_t$	Percentage of oil that can be recovered in the emulsified oil collected at time $t$
$\theta_t$	Percentage of oil removed from the sea surface due to natural weathering process at time $t$
$\Omega_{p',p}$	Collocation matrix
$\Psi_p$	Roots of the Lagrange orthogonal polynomial

### Integer Variables

$x_{i,m,t}^M$	Number of mechanical systems of type $m$ from staging area $i$ operating on scene at time period $t$
$x_{i,b,t}^B$	Number of in-situ burning systems of type $b$ from staging area $i$ operating on scene at time period $t$
$xx_{b,t}^B$	0-1 variable. Equal to 1 if the oil slick is thicker than $THICK_b$
$x_{i,d,t}^D$	Number of sorties of dispersant application systems of type $d$ dispatched from staging area $i$ at time period $t$ to spray dispersants

$z_{i,t}$  0-1 variable. Equal to 1 if the shoreline around staging area  $i$  is protected by boom

### Continuous Variables (0 to $+\infty$ )

$area_t$  Area of oil slick on the surface at the end of time  $t$  ( $m^2$ )  
 $bdep_{i,t}$  Amount of coastal protection booms deployed in staging area  $i$  at time period  $t$  (m)  
 $bfail_{i,t}$  Amount of coastal protection booms failed in staging area  $i$  at time period  $t$  (m)  
 $bl_{i,t}$  Length of coastal protection boom along the shore of staging area  $i$  at the end of time  $t$  (m)  
 $S_{t,p}$  Value of the state in finite element  $t$  and collocation point  $p$   
 $SO_t$  State value at the beginning of finite element  $t$   
 $WM_t$  Volume of oil collected and recovered through mechanical systems at time  $t$  ( $m^3$ )  
 $WB_t$  Volume of oil removed by in-situ burning at time period  $t$  ( $m^3$ )  
 $WD_t$  Volume of oil dispersed due to chemical dispersant application at time period  $t$  ( $m^3$ )  
 $v_t$  Volume of oil on the surface at the end of time  $t$  ( $m^3$ )

### Continuous Variables ( $-\infty$ to $+\infty$ )

$\dot{S}_{t,c}$  First-order derivative of the state

### Nomenclature for the ODE model

$A$  Area of oil slick ( $m^2$ )  
 $A_{ev}$  Constant for oil weathering process (empirical value equals to 6.3)  
 $A_0$  Initial area of slick ( $m^2$ )  
 $AC$  Asphaltene content (%) of the parent oil  
 $B_{ev}$  Constant for oil weathering process (empirical value equals to 10.3)  
 $C_3$  Constant for the oil weathering process ( $\sim 0.7$  for crude oils)  
 $C_4$  Constant for oil weathering process (equal to 10 for crude oils)  
 $F_E$  Fraction of oil evaporated  
 $g$  Acceleration of gravity (equals to  $9.8 \text{ m} \cdot \text{s}^{-2}$ )  
 $K_1$  Constant for oil weathering process (empirical value equals to  $150 \text{ s}^{-1}$  based on ref. )  
 $k_2$  Constant for oil weathering process (empirical value equals to 1.21 by NOAA)  
 $k_3$  Constant for oil weathering process (empirical value equals to 1.53 by NOAA)  
 $K_{em}$  Constant for oil weathering process (empirical value equals to  $1 \times 10^{-6}$ )  
 $K_{ev}$  Mass transfer coefficient for evaporation process  
 $tf_1$  Time when the oil spillage stops (release duration)  
 $tf_2$  Time at the end of the planning horizon (the end of the planning horizon)  
 $T_G$  Gradient of the oil distillation curve (K)  
 $T_K$  Temperature (K)  
 $T_O$  Initial boiling point of oil (K)  
 $V$  Volume of oil slick ( $m^3$ )  
 $V_0$  Initial volume of oil spilled before time 0 ( $m^3$ )  
 $V_D$  Volume of oil naturally dispersed ( $m^3$ )  
 $VI$  Time-dependent oil spill rate ( $m^3 \cdot s^{-1}$ )  
 $WIND$  Wind speed ( $m \cdot s^{-1}$ )  
 $Y_W$  Fraction of water content in the emulsion  
 $\nu_w$  Kinematic viscosity of seawater ( $0.801 \times 10^{-6} \text{ m}^2 \cdot \text{s}^{-1}$  under  $30^\circ\text{C}$ )  
 $\rho_w$  Seawater density ( $\text{kg} \cdot \text{m}^{-3}$ )  
 $\rho_o$  Oil density ( $\text{kg} \cdot \text{m}^{-3}$ )  
 $\mu$  Viscosity of oil slick ( $\text{kg} \cdot \text{m}^{-1} \cdot \text{s}^{-1}$ )  
 $\delta$  Thickness of oil slick (m)  
 $\mu_0$  Viscosity of parent oil ( $\text{kg} \cdot \text{m}^{-1} \cdot \text{s}^{-1}$ )  
 $\zeta_t$  Oil-water interfacial tension ( $\text{N} \cdot \text{m}^{-1}$ )

## References

1. NOAA *Oil spill case histories 1967-1991: summaries of significant U.S. and international spills*; Seattle, Washington, 1992.
2. <http://www.restorethegulf.gov/>.
3. <http://www.deepwaterhorizonresponse.com/>.
4. Wilhelm WE, Srinivasa AV. Prescribing tactical response for oil spill clean up operations. *Management Science*. 1997; 43:386-402.
5. Reed M, Johansen I, Brandvik PJ, Daling P, Alun Lewisà, Fioccoà R, Mackay D, Prentki R. Oil spill modeling towards the close of the 20th century: overview of the state of the art. *Spill Science & Technology Bulletin*. 1999; 5:3-16.
6. Brebbia CA. *Oil spill modeling and processes*. WIT Press: UK, 2001.
7. Fingas M. *The basics of oil spill cleanup*. Lewis: New York, 2001.
8. Ornitz B, Champ M. *Oil spills first principles: prevention and best response*. Elsevier: Netherlands, 2003.
9. Mackay D, Buist IA, Mascarenhas R, Paterson S *Oil spill processes and models: Environment Canada Manuscript Report No 8. EE-8*; Ottawa, Ontario, 1980.
10. Reed M. The physical fates component of the natural resource damage assessment model system. *Oil & Chemical Pollution*. 1989; 5:99-123.
11. Zhong Z, You F. Oil spill response planning with consideration of physicochemical evolution of the oil slick: A multiobjective optimization approach. *Computers & Chemical Engineering*. 2010:Submitted.
12. Fay JA. The spread of oil slicks on a calm sea. In *Oil on the sea*, Hoult D-P, Ed. Plenum Press: New York, 1969; pp 53-63.
13. Sebastiao P, Sores CG. Modeling the fate of oil spills at sea. *Spill Science & Technology Bulletin*. 1995; 2:121-131.
14. Stiver W, Mackay D. Evaporation rate of spills of hydrocarbons and petroleum mixtures. *Environmental Science & Technology*. 1984; 18:834-840.
15. Buchanan I, Hurford N. Methods for predicting the physical changes in oil spilt at sea. *Oil & Chemical Pollution*. 1988; 4:311-328.
16. Ventikos NP, Vergetis E, Psaraftis HN, Triantafyllou G. A high-level synthesis of oil spill response equipment and countermeasures. *Journal of Hazardous Materials*. 2004; 107:51-58.
17. Michel J, Adams EE, Addassi Y, Copeland T, Greeley M, James B, McGee B, Mitchelmore C, Onishi Y, Payne J, Salt D, Wrenn B. *Oil spill dispersants: efficacy and effects*. National Academies Press: Washington, DC, 2005.
18. You F, Grossmann IE. Design of responsive supply chains under demand uncertainty. *Computers & Chemical Engineering*. 2008; 32:2839-3274.
19. You F, Grossmann IE. Balancing responsiveness and economics in the design of process supply chains with multi-echelon stochastic inventory. *AIChE Journal*. 2009; In press:DOI: 10.1002/aic.12244.
20. You F, Grossmann IE. Stochastic inventory management for tactical process planning under uncertainties: MINLP model and algorithms. *AIChE Journal*. 2010; In press:DOI: 10.1002/aic.12338.
21. Biegler LT. Optimization strategies for complex process models. *Advances in Chemical Engineering*. 1992; 18:197-256.
22. Allgor R, Barton P. Mixed-integer dynamic optimization. *Computers & Chemical Engineering*. 1997; 21:S451-S456.
23. Bansal V, Sakizlis V, Ross R, Perkins J, Pistikopoulos E. New algorithms for mixed-integer dynamic optimization. *Computers & Chemical Engineering*. 2003; 27:647-668.
24. Chachuat B, Singer AB, Barton PI. Global methods for dynamic optimization and mixed-integer dynamic optimization. *Industrial & Engineering Chemistry Research*. 2006; 45:8373-8392.
25. Bansal V, Perkins J, Pistikopoulos E. A case study in simultaneous design and control using rigorous, mixed-integer dynamic optimization models. *Industrial & Engineering Chemistry Research*. 2002; 41:760-778.
26. Dua P, Dua V, Pistikopoulos EN. Optimal delivery of chemotherapeutic agents in cancer. *Computers & Chemical Engineering*. 2008; 32:99-107.
27. Giovanoglou A, Barlatier J, Adjiman C, Pistikopoulos E, Cordiner J. Optimal solvent design for batch separation based on economic performance. *AIChE Journal*. 2003; 49:3095-3109.
28. Flores-Tlacuahuac A, Grossmann IE. Simultaneous cyclic scheduling and control of a multiproduct CSTR. *Industrial & Engineering Chemistry Research*. 2006; 45:6698-6712.
29. Flores-Tlacuahuac A, Grossmann IE. Simultaneous scheduling and control of multiproduct continuous parallel lines. *Industrial & Engineering Chemistry Research*. 2010; 49:7909-7921.
30. Flores-Tlacuahuac A, Biegler LT. Simultaneous mixed-integer dynamic optimization for integrated design and control. *Computers & Chemical Engineering*. 2007; 31:588-600.
31. Flores-Tlacuahuac A, Biegler LT. Integrated control and process design during optimal polymer grade transition operations. *Computers & Chemical Engineering*. 2008; 32:2823-2837.

## List of Figure Captions

Figure 1. Major oil transport and weathering processes

Figure 2. Oil spill cleanup and coastal protection operations

Figure 3. Oil spill site and locations of the three staging areas S1, S2, and S3 for the case study

Figure 4. Pareto curve and cost breakdown for case study 1

Figure 5. Time trajectories of the oil volumes removed by three methods and remaining on the sea surface when the response time span is 76 days (Point A in Figure 4, drop lines are for the collocation points in the finite elements)

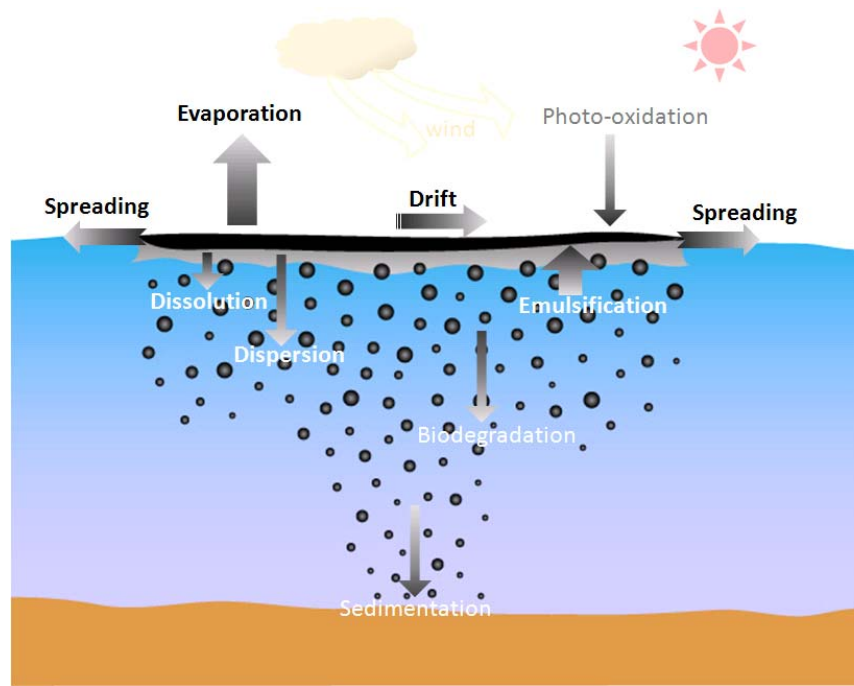
Figure 6. Time trajectories of the oil volumes removed by three methods and remaining on the sea surface when the response time span is 78 days (Point B in Figure 4, drop lines are for the collocation points in the finite elements)

Figure 7. Time trajectories of the oil volumes removed by three methods and remaining on the sea surface when the response time span is 95 days (Point C in Figure 4, drop lines are for the collocation points in the finite elements)

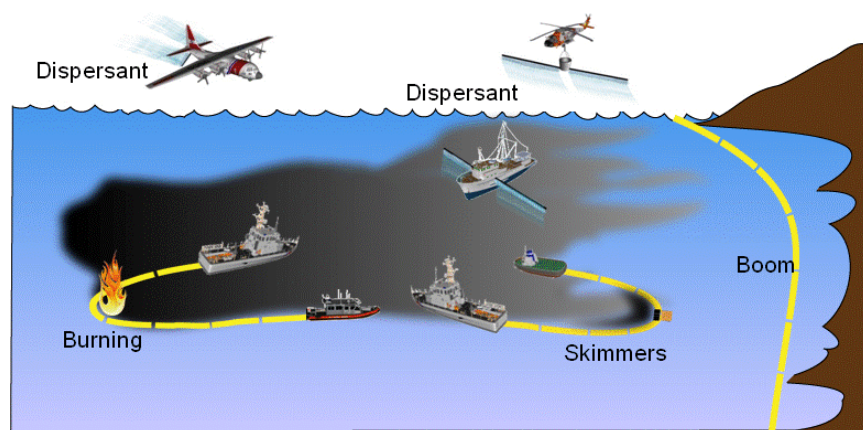
Figure 8. Time trajectories of the oil volumes and area on the sea surface when the response time span is 180 days (Point F in Figure 4, markers are for the collocation points in the finite elements)

Figure 9. Optimal length of coastal protection boom when response time span is 76 days





**Figure 1. Major oil transport and weathering processes**



**Figure 2. Oil spill cleanup and coastal protection operations**

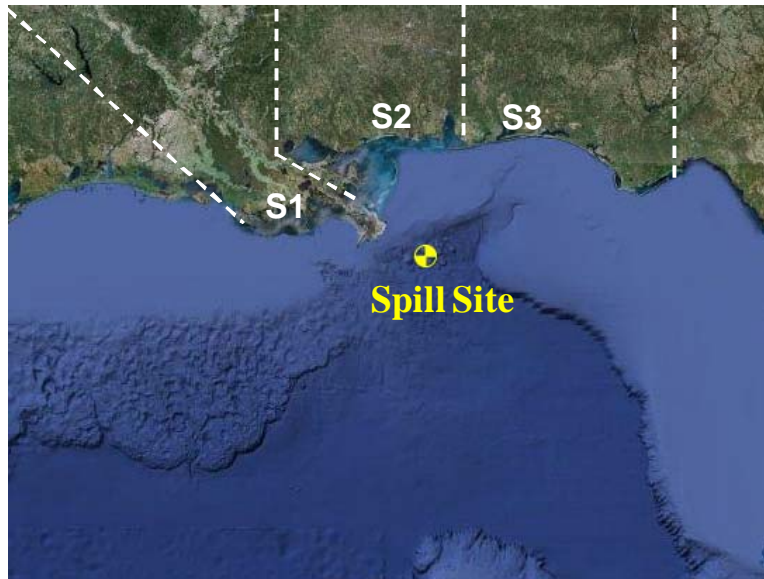


**Figure 3. Oil spill site and locations of the three staging areas S1, S2, and S3 for the case study**

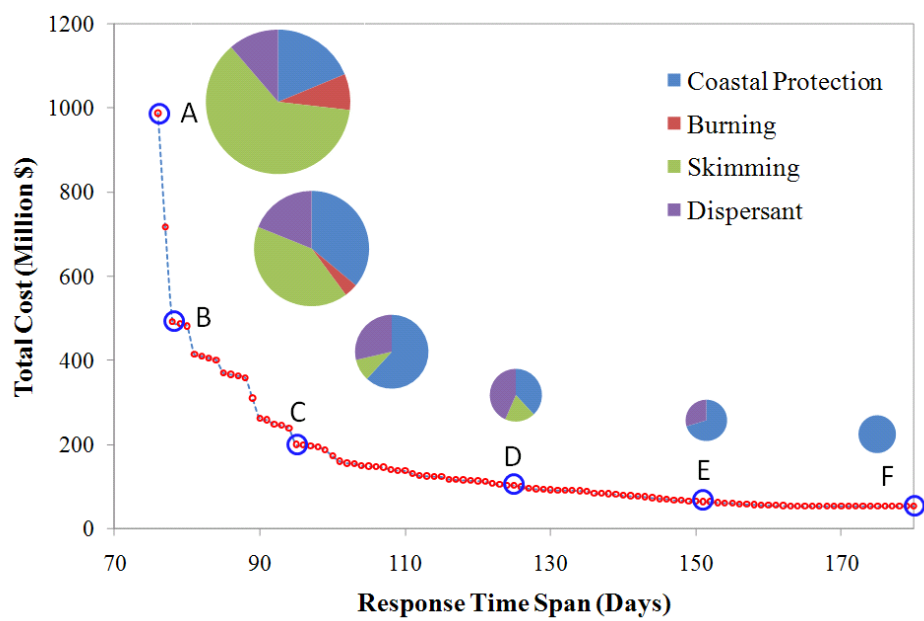


**Figure 4. Pareto curve and cost breakdown for case study 1**

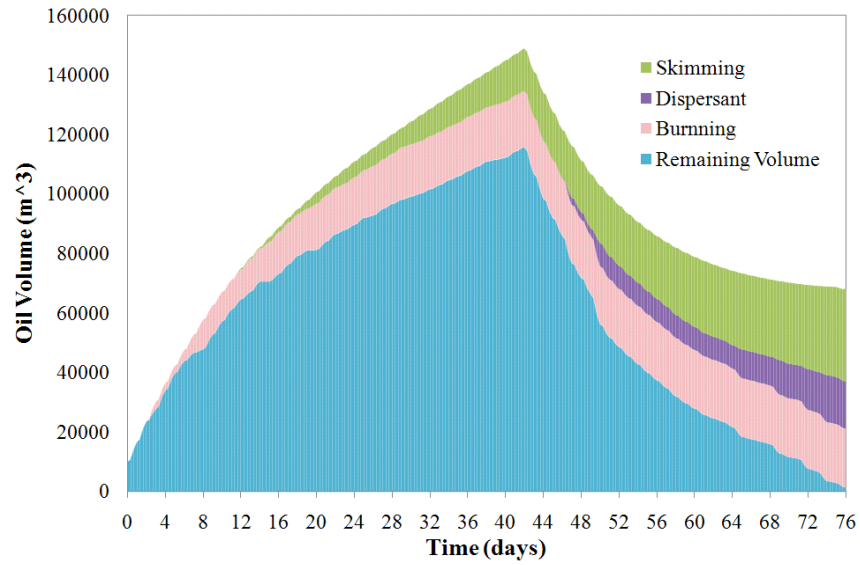


**Figure 5. Time trajectories of the oil volumes removed by three methods and remaining on the sea surface when the response time span is 76 days (Point A in Figure 4, drop lines are for the collocation points in the finite elements)**

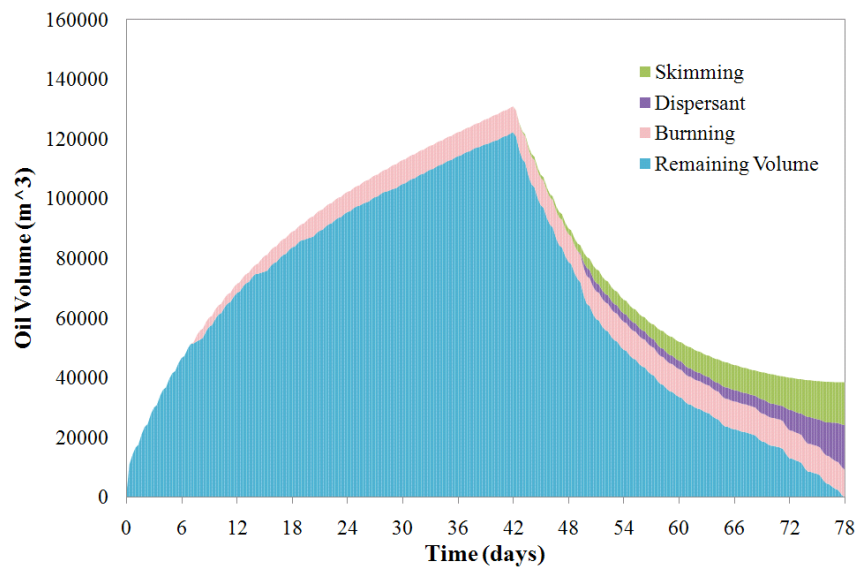


**Figure 6. Time trajectories of the oil volumes removed by three methods and remaining on the sea surface when the response time span is 78 days (Point B in Figure 4, drop lines are for the collocation points in the finite elements)**

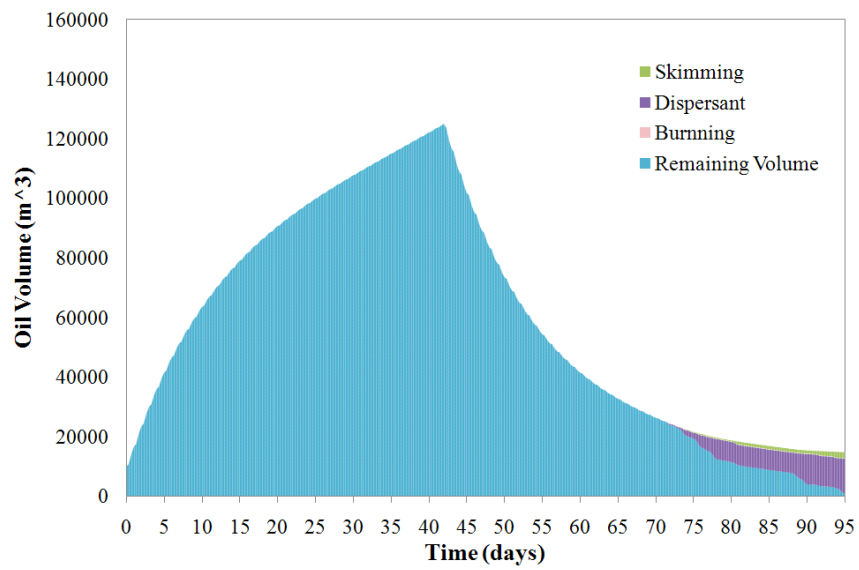


**Figure 7. Time trajectories of the oil volumes removed by three methods and remaining on the sea surface when the response time span is 95 days (Point C in Figure 4, drop lines are for the collocation points in the finite elements)**

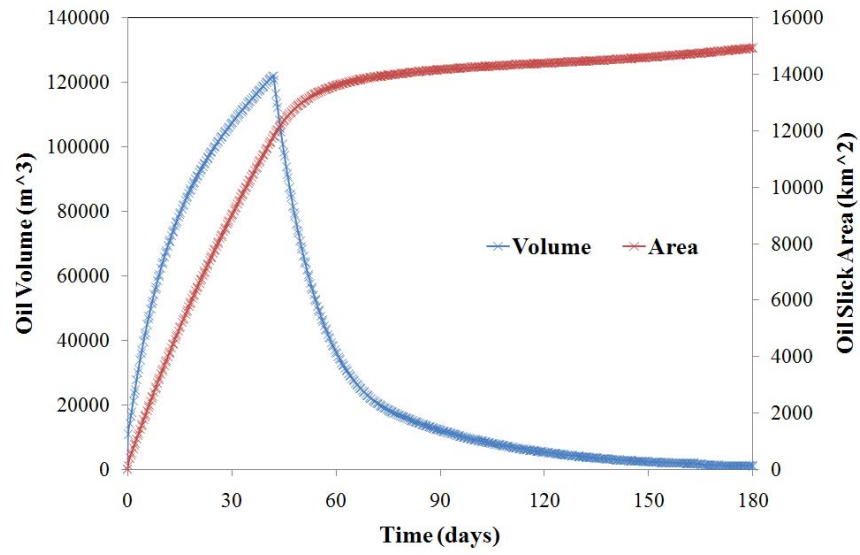


**Figure 8. Time trajectories of the oil volumes and area on the sea surface when the response time span is 180 days (Point F in Figure 4, markers are for the collocation points in the finite elements)**



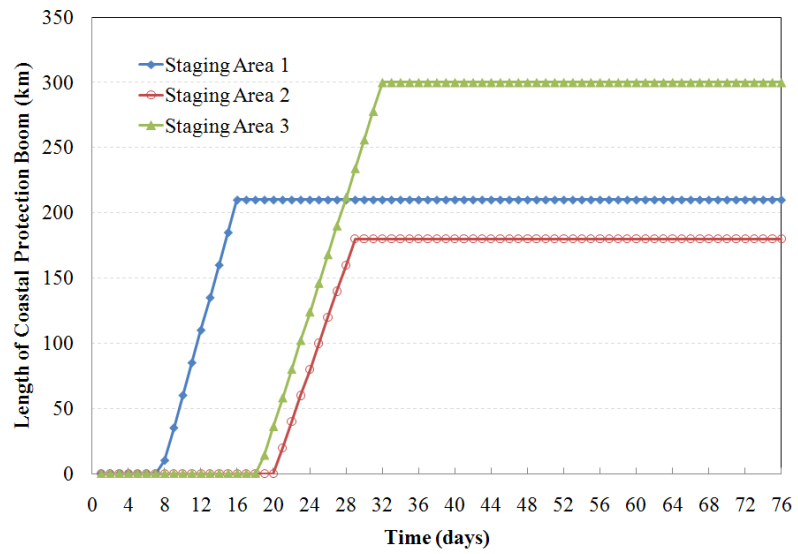


**Figure 9. Optimal length of coastal protection boom when response time span is 76 days**

**Table 1 Input data about cleanup facilities for case study 1**

		S1	S2	S3
Mechanical System Type 1	Cleanup Capacity (m <sup>3</sup> /day)	20	25	30
	Response time (days)	1	2	1
	Availability	20	22	22
Mechanical System Type 2	Cleanup Capacity (m <sup>3</sup> /day)	33	34	35
	Response time (days)	2	1	2
	Availability	20	20	20
Mechanical System Type 3	Cleanup Capacity (m <sup>3</sup> /day)	48	40	50
	Response time (days)	2	2	2
	Availability	20	18	17
In-situ Burning System Type 1	Cleanup Capacity (m <sup>3</sup> /day)	200	230	220
	Response time (days)	3	2	2
	Availability	4	3	4
In-situ Burning System Type 2	Cleanup Capacity (m <sup>3</sup> /day)	340	350	320
	Response time (days)	3	2	3
	Availability	5	4	4
Dispersant Application (Vessel)	Spray Capacity (m <sup>3</sup> /sortie)	1	1	1
	Maximum sorties per day	2	3	3
	Response time (days)	2	1	2
	Availability	7	7	6
Dispersant Application (Helicopter)	Spray Capacity (m <sup>3</sup> /sortie)	1.4	1.1	1.2
	Maximum sorties per day	10	10	9
	Response time (days)	5	4	5
	Availability	5	4	4
Dispersant Application (C-130)	Spray Capacity (m <sup>3</sup> /sortie)	5	6	5
	Maximum sorties per day	7	7	6
	Response time (days)	13	13	14
	Availability	3	3	2